Next-to-leading order QCD and electroweak corrections to Higgs-strahlung processes at the LHC[*]

Pazilet Obul[1,2;1)]   Sayipjamal Dulat[1,2;2)]   Tie-Jiun Hou[1,2]   Ablikim Tursun[1,2]   Nijat Yalkun[1,2]

[1] School of Physics Science and Technology, Xinjiang University, Urumqi, Xinjiang 830046 China
[2] Center for Theoretical Physics, Xinjiang University, Urumqi, Xinjiang 830046 China

Abstract: In this paper we calculate the total and fiducial cross sections as well as differential distributions for the Higgs-strahlung or VH process $pp \to VH \to l\nu_l/l^-l^+ + H$, (V = W or Z, l=e, μ) including QCD and electro-weak corrections up to next-to-leading order before and after reweighting photon PDFs of NNPDF2.3qed, NNPDF3.0qed, MRST2004qed, CT14QEDinc, and LUXqed at the LHC with 13 TeV and Higgs boson mass $M_H = 125$ GeV. The predictions from the various photon PDFs before and after reweighting against each other are in good agreement. The photon PDF uncertainties of the photon-induced cross sections decrease significantly with the reweighting PDFs.

Keywords: Higgs-boson, QCD correction, electro-weak correction, Reweighting-PDFs

PACS: 14.80.Bn, 13.40.Ks, 12.38.-t   **DOI:** 10.1088/1674-1137/42/9/093105

1 Introduction

The Standard Model (SM) predicts the Higgs boson, that is, the remnant of the electroweak (EW) symmetry-breaking mechanism that generates the gauge boson and fermion masses [1]. One of the most important Higgs boson production mechanisms at hadron colliders is the Higgs-strahlung process, i.e. the associated production of Higgs bosons and weak gauge bosons,

$$pp \to WH + X \to H\nu_l l + X \quad \text{and} \quad pp \to ZH + X \to Hl^+l^- + X. \tag{1}$$

In order to determine the Higgs boson properties with high precision at the LHC, it is necessary to calculate the higher order quantum chromodynamics (QCD) and EW corrections. One particular EW correction of interest is that due to photons coming from the proton in the initial state. It is thus necessary to use photon parton distribution functions (PDFs) both for consistency when EW corrections are included, and because photon-induced processes can become important at high energies. So far, a number of PDF groups, namely, the MRST, NNPDF and CTEQ collaborations, have introduced photon PDFs along with PDF evolution at leading order (LO) in QED and next-to-leading order (NLO) or next-to-next-to-leading order (NNLO) in QCD. Reference [2] calcu-lated NLO QCD corrections to the $pp \to W^\pm H + X$ (sum of W^+H and W^-H) and $pp \to ZH + X$ total cross sections at the LHC at 16 TeV and 40 TeV, and discussed in detail the total cross section dependence on the choice of factorization scale and for three different sets of PDFs (MT, KMRS and DFLM) within the DIS scheme and $\overline{MS}$ scheme for $M_H = 100$ GeV. References [3, 4] presented the impact of the EW corrections on the cross section predictions for the processes $pp/p\bar{p} \to W^\pm H + X$ and $pp/p\bar{p} \to ZH + X$ at the Tevatron ($\sqrt{s} = 1.96$ TeV) and LHC ($\sqrt{s} = 14$ TeV) for the three different input parameter schemes (G_μ, $\alpha(M_Z)$, and $\alpha(0)$-schemes), and studied the theoretical uncertainties induced by factorization and renormalization scale dependence and by the PDFs by using the CTEQ6L1 and CTEQ6M [5] PDFs, respectively. The EW corrections in the G_μ and $\alpha(M_Z)$-schemes are significant and reduce the cross section by 5%–9% and by 10%-15%, respectively. The EW corrections in the $\alpha(0)$-scheme are rather small. References [4, 6] discussed the NNLO QCD, i.e. the $O(\alpha_s^2)$, corrections to the $pp/p\bar{p} \to W^\pm H$ and $pp/p\bar{p} \to ZH$ production cross sections at the Tevatron at 1.96 TeV and LHC at 14 TeV for Higgs boson masses $M_H \lesssim 200-300$ GeV using the MRST [7] PDFs. For $M_H = 120$ GeV, the renormalization and factorization scale uncertainty at the LHC at 14 TeV drops from 10% at LO to 5% at

NLO, and to 2% at NNLO. At the Tevatron and for the same Higgs boson mass, the scale uncertainty drops from 20% at LO to 7% at NLO, and to 3% at NNLO. A. Denner et al [8] have discussed the impact of EW radiative corrections to the Higgs-strahlung processes at the Tevatron (1.96 TeV) and LHC (7 TeV and 14 TeV) within the G_μ-scheme for $M_\mathrm{H} = 120$ GeV using the HAWK Monte Carlo program. The LHC Higgs Cross Section Working Group [9] provided an update of the total and fiducial cross-section, together with theoretical uncertainties from renormalization and factorization scales, of the process pp$\to$W$^\pm$/Z+H$\to$lν_l/l$^+$l$^-$+H including NNLO QCD and NLO EW corrections for different proton-proton collision energies ($\sqrt{s}$=7 TeV, 8 TeV, 13 TeV, 14 TeV) for a Higgs boson mass $M_\mathrm{H} = 125$ GeV. Ref. [10] studied the impact of the CMS measurements of W boson pair production at the LHC at 8 TeV on the NNPDF2.3qed, NNPDF3.0qed [11], CT14QEDinc [12], and LUXqed [13] photon PDFs, and found that the data strongly suggest that the NNPDF photon error band should be significantly reduced. Therefore, it is necessary to re-examine the physics effects induced by photon-initiated process. In this paper, by using various PDFs, we update the predictions for the processes pp$\to$W$^\pm$/Z+H$\to$lν_l/l$^+$l$^-$+H

at the LHC at 13 TeV and Higgs boson mass $M_\mathrm{H} = 125$ GeV, including the NLO QCD and EW corrections using the most recent PDFs.

The paper is organized as follows. In Section 2, first we give the Feynman diagrams for the Higgs-strahlung processes pp$\to$W$^\pm$/Z+H$\to$lν_l/l$^+$l$^-$+H at LO and NLO. Then we provide our numerical results for these processes at the LHC with center-of-mass energy 13 TeV using the Monte Carlo program HAWK [14] by adopting the NNPDF2.3qed, NNPDF3.0qed, MRST2004qed, CT14QEDinc, and NNLO LUXqed PDFs, as well as their reweighting photon PDFs. We obtain reweighting photon PDFs by using the reweighting method [15–18] and the LHC CMS 8 TeV data [19] as in Ref. [10]. Our conclusion is given in Section 3.

2   Results

2.1   Feynman diagrams

The LO Feynman diagrams for Higgs boson production in association with weak gauge bosons V = W$^\pm$, Z, at the proton-antiproton collider Tevatron and proton-proton collider LHC, are shown in Fig. 1.
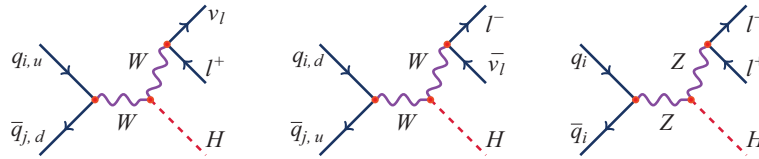

Fig. 1.   (color online) Feynman diagram for Higgs-strahlung processes at LO. The straight, wavy, and dashed lines denote fermions, weak gauge bosons, and Higgs boson, respectively.

The corresponding partonic processes are $\mathrm{q}_{i,\mathrm{u}} \bar{\mathrm{q}}_{j,\mathrm{d}} \to \mathrm{HW}^+ \to \mathrm{H}l^+\nu_\mathrm{l}$ and $\mathrm{q}_{i,\mathrm{d}} \bar{\mathrm{q}}_{j,\mathrm{u}} \to \mathrm{HW}^- \to \mathrm{H}l^-\bar{\nu}_\mathrm{l}$, where $\mathrm{q}_{i,\mathrm{u}}$ and $\mathrm{q}_{i,\mathrm{d}}$ denote up- and down-type quarks of the ith generation, as well as $\mathrm{q}_i \bar{\mathrm{q}}_i \to \mathrm{HZ} \to \mathrm{H}l^+l^-$, where q_i denotes any light quark of the ith generation.

At NLO the corrections to the Higgs-strahlung process includes QCD corrections (virtual corrections with gluon exchange in the q$\bar{\mathrm{q}}$ vertex, gluon-induced processes, and the emission of an additional gluon) and complete EW corrections (incoming photon corrections, virtual and real EW corrections including the outgoing photon corrections). The representative Feynman diagrams for the NLO QCD and EW corrections are shown in Figs. 2, 3 and 4. The EW virtual corrections can be classified into vertex and box corrections.

In this section, we present numerical results for total and differential cross sections for associated W$^\pm$H (W$^+\to$l$^+\nu_\mathrm{l}$ and W$^-\to$l$^-\bar{\nu}_\mathrm{l}$, where l=e,μ) and ZH (Z$\to$

l$^+$l$^-$) production with NNPDF2.3qed, NNPDF3.0qed, MRS2004qed, CT14QEDinc, and LUXqed photon PDFs at the LHC at 13 TeV including the NLO QCD and EW corrections.

2.2   Input parameters and cuts

In our numerical analysis of the VH processes (V = W$^\pm$, Z) we use the same VH input parameters and cuts as in Ref. [9],

$$G_\mathrm{F} = 1.166378\times10^{-5}\ \mathrm{GeV}^{-2},\ \alpha_\mathrm{s}(M_\mathrm{Z}) = 0.11801,$$

$$\Gamma_\mathrm{W} = 2.08430\ \mathrm{GeV},\ \Gamma_\mathrm{Z} = 2.49427\ \mathrm{GeV},$$

$$M_\mathrm{H} = 125\ \mathrm{GeV},\ M_\mathrm{W} = 80.35797\ \mathrm{GeV},\ M_\mathrm{Z} = 91.15348\ \mathrm{GeV},$$

$$m_\mathrm{e} = 0.510998910\ \mathrm{MeV},\ m_\mathrm{\mu} = 0.105658\ \mathrm{GeV},$$

$$m_\mathrm{t} = 172.5\ \mathrm{GeV}$$

Self-energy diagrams:
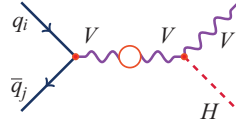
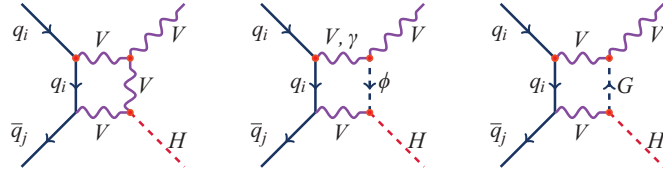Vertex diagrams:
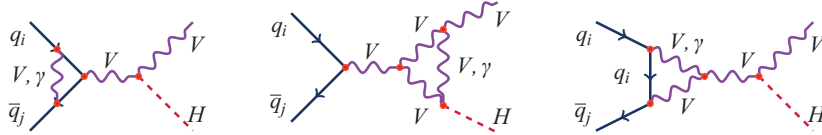
Box diagrams:

Fig. 2.   (color online) Feynman diagrams corresponding to the EW virtual corrections to the LO processes.
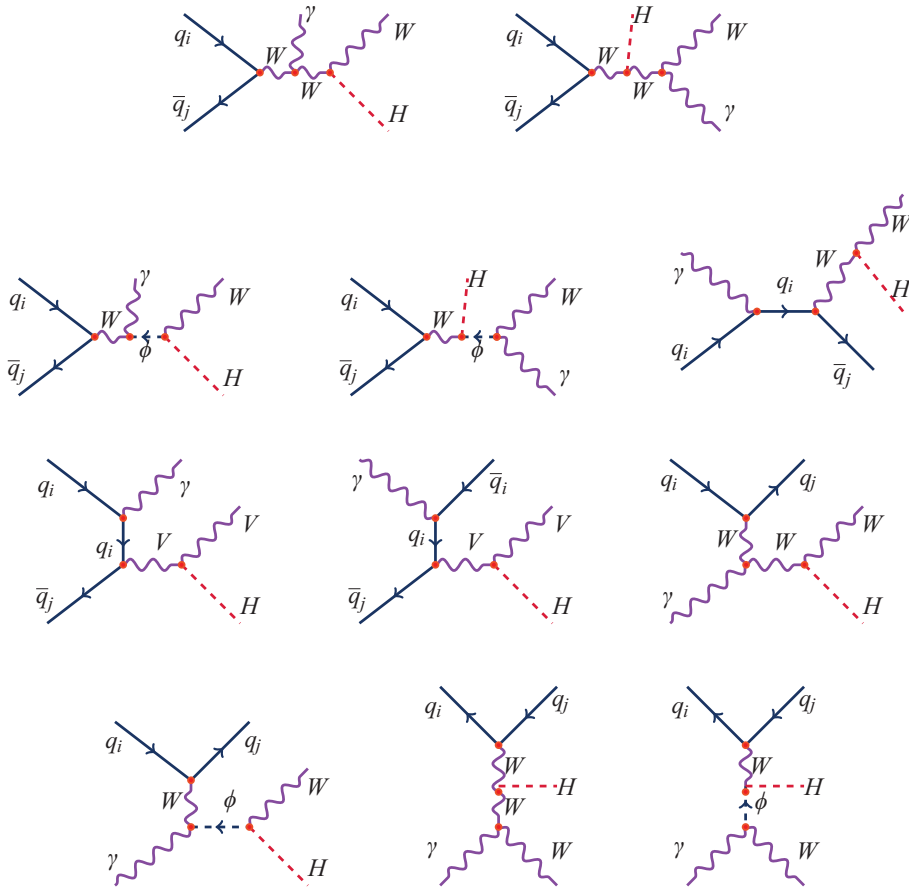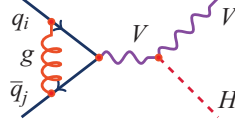

Fig. 3.   (color online) Feynman diagrams corresponding to the EW real corrections to the LO processes.
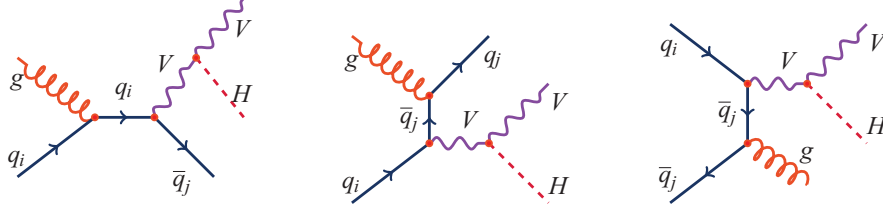
(a)Virtual diagrams:

(b)Real diagrams:

Fig. 4.   (color online) Feynman diagrams corresponding to the NLO QCD corrections to the LO processes.

The electromagnetic coupling is fixed in the G_{F}-scheme,

$$\alpha_{G_{\mathrm{F}}} = \frac{\sqrt{2} G_{\mathrm{F}} M_{\mathrm{W}}^2}{\pi} \sin^2 \theta_{\mathrm{W}} \qquad (2)$$

and the weak mixing angle is defined in the on-shell scheme,

$$\sin^2 \theta_{\mathrm{W}} = 1 - M_{\mathrm{W}}^2 / M_Z^2. \qquad (3)$$

Both the factorization and the renormalization scales are set to the value of the invariant mass of the VH system,

$$\mu = \mu_{\mathrm{R}} = \mu_{\mathrm{F}} = M_{\mathrm{VH}}, \; M_{\mathrm{VH}}^2 \equiv (p_{\mathrm{V}} + p_{\mathrm{H}})^2. \qquad (4)$$

We also provide results for the total cross section and differential cross section in the same kinematic region as in Ref. [9],

$$p_{T_1} > 15 \text{ GeV}, \qquad |y_1| < 2.5, \qquad (5)$$

where p_{T_1} is the transverse momentum of the lepton and y_1 is its rapidity. For $Z(\to l^+ l^-)H$ production the invariant mass of the two leptons is in the range

$$75 \text{ GeV} < M_{\mathrm{ll}} < 105 \text{ GeV}. \qquad (6)$$

2.3   Total cross sections

First we study the effect of the NLO corrections on the LO cross sections without any cuts on the final-state charged leptons using the SM input parameters given in Section 2.2. The total NLO VH cross sections $\sigma_{\mathrm{NLO}}^{\mathrm{VH}}$ and relative corrections $\delta_{\mathrm{QCD/EW}}$ are calculated according to

$$\sigma_{\mathrm{NLO}}^{\mathrm{VH}} = \sigma_{\mathrm{LO}}^{\mathrm{VH}} (1 + \delta_{\mathrm{EW}} + \delta_{\mathrm{QCD}}) + \sigma_\gamma, \qquad (7)$$

and

$$\delta_{\mathrm{QCD/EW}} = \frac{\sigma_{\mathrm{QCD/EW}}}{\sigma_{\mathrm{LO}}^{\mathrm{VH}}} \times 100\%. \qquad (8)$$

For the LO calculations, strictly speaking, one should use LO PDFs, but for convenience, we used NLO PDFs. In Tables 1, 2, and 3 we list the LO and NLO total cross sections (σ_{LO}, σ_{NLO}) including NLO QCD and EW corrections (δ_{QCD}, δ_{EW}), and photon-induced cross sections (σ_γ, $\sigma_{\gamma \mathrm{PR}}$) with PDF uncertainties for the Higgs-strahlung processes $pp \to W^\pm / Z + H \to l\nu_l / l^+ l^- + H$ with NNPDF2.3qed, NNPDF3.0qed, MRS2004qed, CT14QEDinc, and LUXqed photon PDFs and Higgs-boson mass $M_{\mathrm{H}} = 125$ GeV at the LHC at $\sqrt{s} = 13$ TeV. The photon-induced cross section is only significant for WH production. Note that we did not apply reweighting to the LUXqed photon PDFs since the PDF uncertainty of the photon-induced cross section is already small. We see from Tables 1 and 2 that the photon-induced cross section σ_γ and uncertainties depend on the choice of the photon PDFs. Especially, the photon PDF uncertainties decrease significantly as we change from NNPDF2.3qed and NNPDF3.0qed to MRST2004qed, CT14QEDinc, and to LUXqed. The NLO QCD corrections for various photon PDFs are of the order of $+17.0\%$ for total cross sections. The EW corrections are insensitive to the choice of the photon PDFs, and are about -7.0%. The reweighting PDF uncertainties of the photon-induced cross section $\sigma_{\gamma \mathrm{PR}}$ are reduced significantly after including the CMS data to reweight the NNPDF2.3qed, NNPDF3.0qed, MRS2004qed, and CT14QEDinc photon PDFs, while the corresponding central predicted cross sections are unchanged. From Table 1 ($pp \to H + W^+ (\to l^+ \nu_l)$), the relative errors $\Delta \sigma_\gamma / \sigma_\gamma$ for the photon-induced cross sections reduce from 88.7% and 89.5% in the NNPDF2.3qed and NNPDF3.0qed predictions to 5.5% and 8.2% in the reweighting NNPDF2.3qed and reweighting NNPDF3.0qed predictions; the relative

Table 1.   The first and second rows are the total cross sections in LO and NLO; the third row is the photon-induced process cross sections; and the fourth and fifth rows are the NLO QCD and EW corrections and corresponding PDF uncertainties (68% CL) for the process pp→H+W$^+$($\to l^+\nu_l$) with various PDFs at the LHC at 13 TeV and Higgs boson mass M_H=125 GeV without kinematic cuts. The last row is the photon-induced process cross sections and PDF uncertainties for the various re-weighted PDFs.

PDF	NNPDF2.3qed	NNPDF3.0qed	MRST2004qed	CT14QEDinc	LUXqed
σ_{LO}/fb	79.06±1.15	78.45±1.17	78.75±0.03	78.75±0.07	80.59±0.13
σ_{NLO}/fb	93.66±5.70	92.30±5.56	92.43±0.61	90.48±0.27	93.36±0.15
σ_γ/fb	6.01±5.33	5.94±5.32	4.46±0.65	4.47±0.36	4.49±0.006
δ_{QCD}(%)	17.53±0.04	17.47±0.05	17.75±0.005	17.39±0.001	17.68±0.008
δ_{EW}(%)	−7.41±0.008	−7.43±0.009	−7.42±0.006	−7.41±0.006	−7.41±0.001
$\sigma_{\gamma PR}$/fb	6.01±0.33	5.94±0.49	4.46±0.21	4.47±0.19	4.49±0.006

Table 2.   The first and second rows are the total cross sections in LO and NLO; the third row is the photon-induced process cross sections; and the fourth and fifth rows are the NLO QCD and EW corrections and corresponding PDF uncertainties (68% CL) for the process pp→H+W$^-$($\to l^-\bar\nu_l$) with various PDFs at the LHC at 13 TeV and Higgs boson mass M_H=125 GeV without kinematic cuts. The last row is the photon-induced process cross sections and PDF uncertainties for the various re-weighted PDFs.

PDF	NNPDF2.3qed	NNPDF3.0qed	MRST2004qed	CT14QEDinc	LUXqed
σ_{LO}/fb	50.41±0.73	49.77±0.85	49.35±0.02	49.73±0.06	51.36±0.09
σ_{NLO}/fb	59.41±4.27	58.65±4.23	57.78±0.41	56.99±0.14	59.35±0.11
σ_γ/fb	4.19±4.05	4.18±3.99	2.89±0.43	2.86±0.20	2.98±0.004
δ_{QCD}(%)	16.79±0.06	16.73±0.05	17.05±0.005	16.79±0.002	17.02±0.008
δ_{EW}(%)	−7.26±0.007	−7.30±0.0006	−7.28±0.0005	−7.28±0.006	−7.26±0.001
$\sigma_{\gamma PR}$/fb	4.19±0.24	4.18±0.40	2.89±0.13	2.86±0.11	2.98±0.004

Table 3.   The first and second rows are the total cross sections in LO and NLO; the third row is the photon-induced process cross sections; and the fourth and fifth rows are the NLO QCD and EW corrections and corresponding PDF uncertainties (68% CL) for the process p p→H+Z($\to l^+l^-$) with various PDFs at the LHC at 13 TeV and Higgs boson mass M_H = 125 GeV. The last row is the photon-induced process cross sections and corresponding PDF uncertainties for the various re-weighted PDFs.

PDF	NNPDF2.3qed	NNPDF3.0qed	MRST2004qed	CT14QEDinc	LUXqed
σ_{LO}/fb	21.77±0.31	21.58±0.32	21.72±0.0006	21.68±0.02	22.26±0.03
σ_{NLO}/fb	24.74±0.56	24.46±0.51	24.65±0.02	24.47±0.006	25.19±0.04
σ_γ/fb	0.42±0.32	0.37±0.32	0.29±0.03	0.30±0.02	0.29±0.0003
δ_{QCD}(%)	16.82±0.05	16.71±0.05	17.02±0.005	16.79±0.002	17.00±0.009
δ_{EW}(%)	−5.14±0.005	−5.13±0.005	−5.10±0.002	−5.16±0.0002	−5.15±0.0008
$\sigma_{\gamma PR}$/fb	0.42±0.02	0.37±0.03	0.29±0.006	0.30±0.006	0.29±0.0003

errors $\Delta\sigma_\gamma/\sigma_\gamma$ reduce from 23.9% in the MRST2004qed predictions to 7.6% in the reweighting MRST2004qed predictions; the relative errors $\Delta\sigma_\gamma/\sigma_\gamma$ reduce from 13.4% in the CT14QEDinc predictions to 7.1% in the reweighting CT14QEDinc predictions.

From Table 2 (pp → H + W$^-$($\to$ l$^-\bar\nu_l$)) we see that the relative errors $\Delta\sigma_\gamma/\sigma_\gamma$ of the photon-induced cross sections reduce from 96.6% and 95.4%

in the NNPDF2.3qed and NNPDF3.0qed predictions to 5.7% and 9.5% in the reweighting NNPDF2.3qed and reweighting NNPDF3.0qed predictions; the relative errors $\Delta\sigma_\gamma/\sigma_\gamma$ reduce from 24.5% in the MRST2004qed predictions to 7.6% in the reweighting MRST2004qed predictions; and the relative errors $\Delta\sigma_\gamma/\sigma_\gamma$ reduce from 11.8% in the CT14QEDinc predictions to 6.3% in the reweighting CT14QEDinc predictions.

From Table 3 (pp→H+Z(→l$^+$l$^-$)) we see that the photon-induced cross section contributions is small for various photon PDFs; the NLO QCD corrections are of the order of +17% for total cross sections; the EW corrections are insensitive to the choice of the PDF set, and are about −5%; the PDF uncertainties of the photon-induced cross sections $\sigma_{\gamma PR}$ are reduced significantly after including the CMS data to reweight the various photon PDFs, while the average predicted cross sections are unchanged. For example, the relative errors $\Delta\sigma_\gamma/\sigma_\gamma$ of the photon-induced cross sections reduce from 76.2% and 86.5% in the NNPDF2.3qed and NNPDF3.0qed predictions to 4.7% and 8.1%; in the reweighting NNPDF2.3qed and reweighting NNPDF3.0qed predictions; the relative errors $\Delta\sigma_\gamma/\sigma_\gamma$ reduce from 17.2% in the MRST2004qed predictions to 5.1% in the reweighting MRST2004qed predictions; and the relative errors $\Delta\sigma_\gamma/\sigma_\gamma$ reduce from 10.1% in the CT14QEDinc predictions to 3.7% in the reweighting CT14QEDinc predictions.

2.4   Fiducial cross section

Apart from the total cross section without any cuts, in this subsection we consider the total cross section after applying cuts to the charged leptons. In Tables 4, 5, and 6 we list the LO and NLO total cross sections ($\sigma_{\rm LO}$, $\sigma_{\rm NLO}$) including NLO QCD and EW corrections ($\delta_{\rm QCD}$, $\delta_{\rm EW}$), and photon-induced cross sections (σ_γ, $\sigma_{\gamma PR}$) with PDF uncertainties for the Higgs-strahlung processes pp→W$^\pm$/Z+H→lν_l/l$^+$l$^-$+H with kinematical cuts in Section 2.2 with NNPDF2.3qed, NNPDF3.0qed, MRS2004qed, CT14QEDinc, and LUXqed photon PDFs and Higgs boson mass $M_{\rm H}$=125 GeV at the LHC with $\sqrt{s}$=13 TeV. The LO and NLO total cross sections are reduced by the kinematical cuts. The NLO QCD cor-

rections for VH do not depend on the cuts on the final state charged lepton, but the EW corrections and the photon-induced cross section do depend on them. The photon-induced cross section is only significant for WH production. It is about 10^{-3} fb for the pp→H+Z(→l$^+$l$^-$) process, as we can see from Table 6. Note that we did not apply reweighting to the LUXqed photon PDFs, since the PDF uncertainty of the photon-induced cross section is already small. The NLO QCD corrections for various photon PDFs are of the order of +17.0% for total cross sections. The EW corrections are insensitive to the choice of the photon PDFs, and are about −8.0% for W$^+$H, −7.0% W$^-$H and −9.0% for ZH with leptonic decays. We see from Tables 4 and 5 that the photon-induced cross sections σ_γ and uncertainties depend on the choice of the photon PDFs. Especially, the photon PDF uncertainties decrease significantly as we change from NNPDF2.3qed and NNPDF3.0qed to MRST2004qed, CT14QEDinc, and to LUXqed. The reweighting PDF uncertainties of the photon-induced cross sections $\sigma_{\gamma PR}$ are reduced significantly after including the CMS data to reweight the NNPDF2.3qed, NNPDF3.0qed, MRS2004qed, and CT14QEDinc photon PDFs, while the corresponding central predicted cross sections are unchanged. From Table 4 (pp → H+W$^+$(→l$^+\nu_l$)) we see that the relative errors $\Delta\sigma_\gamma/\sigma_\gamma$ for the photon-induced cross sections reduce from 55.5% and 58.7% in the NNPDF2.3qed and NNPDF3.0qed predictions to 10.5% and 7.2% in the reweighting NNPDF2.3qed and reweighting NNPDF3.0qed predictions; the relative errors $\Delta\sigma_\gamma/\sigma_\gamma$ reduce from 21.6% in the MRST2004qed predictions to 6.6% in the reweighting MRST2004qed predictions; the relative errors $\Delta\sigma_\gamma/\sigma_\gamma$ reduce from 10.6% in the CT14QEDinc predictions to 5.5% in the reweighting CT14QEDinc predictions.

Table 4.   The first and second rows are the fiducial cross sections in LO and NLO; the third row is the photon-induced process fiducial cross sections; and the fourth and fifth rows are the NLO QCD and EW corrections and corresponding PDF uncertainties (68% CL) for the process pp→H+W$^+$(→l$^+\nu_l$) with various PDFs at the LHC at 13 TeV and Higgs boson mass $M_{\rm H}$=125 GeV without kinematic cuts. The last row is the photon-induced process fiducial cross sections and PDF uncertainties with various re-weighted PDFs.

PDF	NNPDF2.3qed	NNPDF3.0qed	MRST2004qed	CT14QEDinc	LUXqed
$\sigma_{\rm LO}$/fb	65.09±0.96	64.61±0.98	64.59±0.03	64.78±0.07	66.33±0.11
$\sigma_{\rm NLO}$/fb	73.64±1.80	72.94±1.90	73.58±0.29	72.95±0.09	75.05±0.12
σ_γ/fb	2.56±1.42	2.35±1.38	2.40±0.32	2.54±0.16	2.51±0.003
$\delta_{\rm QCD}$(%)	17.41±0.04	17.41±0.04	17.69±0.003	17.36±0.02	17.57±0.007
$\delta_{\rm EW}$(%)	−8.27±0.01	−8.18±0.008	−8.24±0.0002	−8.26±0.01	−8.21±0.001
$\sigma_{\gamma PR}$/fb	2.56±0.27	2.35±0.17	2.40±0.10	2.54±0.09	2.51±0.003

Table 5.   The first and second rows are the fiducial cross sections in LO and NLO; the third row is the photon-induced process fiducial cross sections; the fourth and fifth rows are the NLO QCD and EW corrections and corresponding PDF uncertainties (68% CL) for the process pp→H+W$^-$($\to$l$^-\bar{\nu}_l$) with various PDFs at the LHC at 13 TeV and Higgs boson mass M_H=125 GeV without kinematic cuts.

PDF	NNPDF2.3qed	NNPDF3.0qed	MRST2004qed	CT14QEDinc	LUXqed
σ_{LO}/fb	37.70±0.52	37.25±0.62	37.23±0.18	37.33±0.04	38.46±0.07
σ_{NLO}/fb	42.96±1.16	42.29±1.25	42.62±0.18	42.22±0.04	43.74±0.08
σ_γ/fb	1.65±0.95	1.49±0.93	1.44±0.19	1.51±0.11	1.54±0.002
δ_{QCD}(%)	17.42±0.06	17.38±0.05	17.66±0.005	17.42±0.004	17.60±0.007
δ_{EW}(%)	−7.96±0.008	−7.87±0.008	−7.95±0.0002	−7.94±0.006	−7.89±0.001
$\sigma_{\gamma\mathrm{PR}}$/fb	1.65±0.17	1.49±0.11	1.44±0.06	1.51±0.05	1.54±0.002

Table 6.   The first and second rows are the fiducial cross sections in LO and NLO; the third row is the photon-induced process fiducial cross sections; and the fourth and fifth rows are the NLO QCD and EW corrections and corresponding PDF uncertainties (68% CL) for the process p p→H+Z($\to$l$^+$l$^-$) with various PDFs at the LHC at 13 TeV and Higgs boson mass M_H=125 GeV.

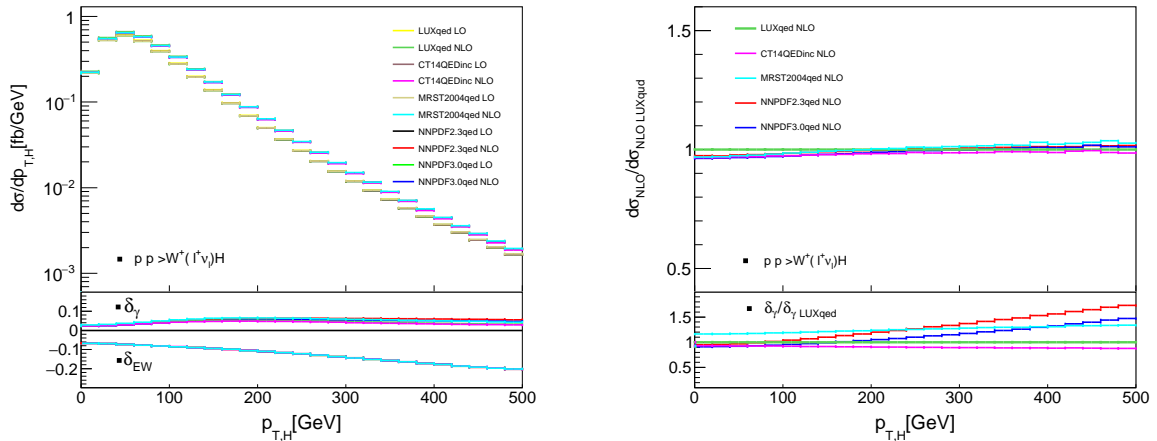| PDF	NNPDF2.3qed	NNPDF3.0qed	MRST2004qed	CT14QEDinc	LUXqed
σ_{LO}/fb	13.50±0.18	13.64±0.20	13.48±0.006	13.44±0.01	14.05±0.02
σ_{NLO}/fb	14.63±0.20	14.76±0.22	14.65±0.006	14.58±0.02	15.24±0.02
σ_γ/fb	1×10^{-3}	6×10^{-3}	2×10^{-3}	2×10^{-3}	7×10^{-3}
δ_{QCD}(%)	17.37±0.05	17.30±0.04	17.67±0.003	17.45±0.003	17.53±0.009
δ_{EW}(%)	−9.01±0.008	−9.15±0.008	−9.01±0.0002	−8.99±0.004	−9.15±0.001

Fig. 5.   (color online) Fiducial differential cross section distributions (top left panel) both at LO (lower curves) and NLO (upper curves) and ratio of dσ_{NLO}/d$\sigma_{\mathrm{NLOLUXqed}}$ (top right panel) of the Higgs boson in W$^+$(l$^+\nu_l$)H production after applying the selection cuts in Section **2.2** at the LHC at 13 TeV for the various PDFs. The bottom left panel shows the electroweak δ_{EW} and photon corrections δ_γ = dσ_γ/dσ_{LO}. The bottom right panel is the ratio of δ_γ/$\delta_{\gamma\mathrm{LUXqed}}$.
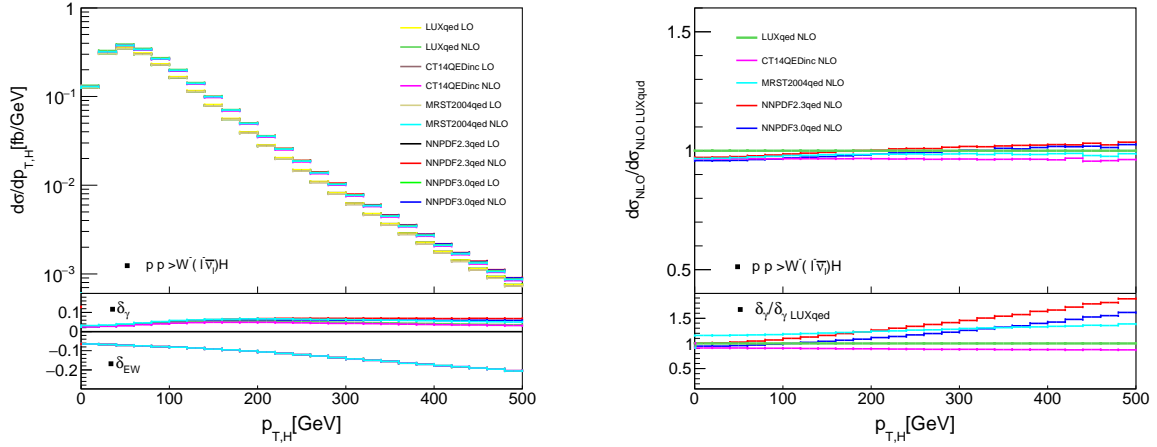
Fig. 6.   (color online) Differential cross section distributions (top left panel) both at LO (lower curves) and NLO (upper curves) and ratio of $d\sigma_{NLO}/d\sigma_{NLOLUXqed}$ (top right panel) of the Higgs boson in $W^-(l^-\bar{\nu}_l)H$ production after applying the selection cuts in section 2.2 at the LHC at 13 TeV for the various PDFs. The bottom left panel shows the electroweak δ_{EW} and photon corrections $\delta_\gamma = d\sigma_\gamma/d\sigma_{LO}$. The bottom right panel is the ratio of $\delta_\gamma/\delta_{\gamma LUXqed}$.
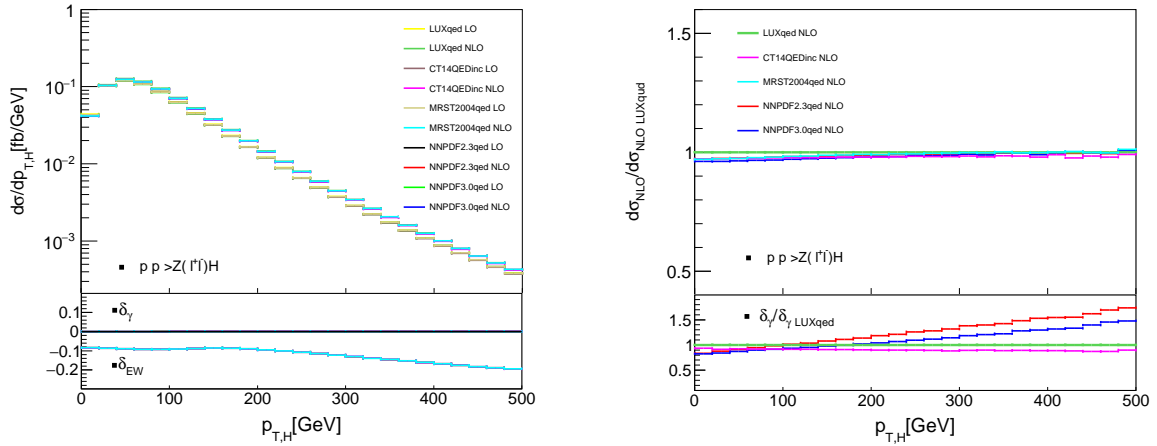

Fig. 7.   (color online) Differential cross section distributions (top left panel) both at LO (lower curves) and NLO (upper curves) and ratio of $d\sigma_{NLO}/d\sigma_{NLOLUXqed}$ (top right panel) of the Higgs boson in $Z(l^+l^-)H$ production after applying the selection cuts in section 2.2 at the LHC at 13 TeV for the various PDFs. The bottom left panel shows the electroweak δ_{EW} and photon corrections $\delta_\gamma = d\sigma_\gamma/d\sigma_{LO}$. The bottom right panel is the ratio of $\delta_\gamma/\delta_{\gamma LUXqed}$.

From Table 5 ($pp \to H + W^-(\to l^- \bar{\nu}_l)$) we see that the relative errors $\Delta\sigma_\gamma/\sigma_\gamma$ for the photon-induced cross section reduce from 57.6% and 62.4% in the NNPDF2.3qed and NNPDF3.0qed predictions to 10.3% and 7.4% in the reweighting NNPDF2.3qed and reweighting NNPDF3.0qed predictions; the relative errors $\Delta\sigma_\gamma/\sigma_\gamma$ reduce from 22.2% in the MRST2004qed predictions to 6.9% in the reweighting MRST2004qed predictions; and the relative errors $\Delta\sigma_\gamma/\sigma_\gamma$ reduce from 11.3% in the CT14QEDinc predictions to 5.9% in the reweighting

CT14QEDinc predictions.

2.5   Fiducial differential cross section

In this subsection we consider the differential cross sections after applying cuts to the charged leptons. We plot the transverse-momentum distributions for Higgs production in $pp \to W^\pm/Z + H \to l\nu_l/l^+l^- + H$ at LO and NLO in QCD for Higgs boson mass $M_H = 125$ GeV with the kinematical cuts and set up described in Section 2.2.

The $p_{\mathrm{T}}(\mathrm{H})$ distributions of the Higgs boson are shown in Figs. 5, 6 and 7 for various PDFs. From the NLO (upper) and LO (lower) $p_{\mathrm{T}}(\mathrm{H})$ distribution curves we see that the NLO correction is small at small $p_{\mathrm{T}}(\mathrm{H})$, and increases slightly with $p_{\mathrm{T}}(\mathrm{H})$ as the cross section falls rapidly. The upper left plot is the transverse-momentum distributions of Higgs boson production at LO (lower curves) and NLO (upper curves) including NLO QCD and EW corrections. The lower left plot is the photon correction $\delta_{\gamma} = \mathrm{d}\sigma_{\gamma}/\mathrm{d}\sigma_{\mathrm{LO}}$ and EW corrections δ_{EW} for various PDFs. The EW correction for the process pp→H+W(→lν$_{\mathrm{l}}$) grows further negative to (10–20)% as $p_{\mathrm{T}}(\mathrm{H})$ increases. The photon-induced corrections have a tendency to grow as well, but can reach only 2.5% level. In the top right plot we show transverse-momentum distributions of various PDF predictions to LUXqed prediction. The bottom right panel is the ratio of $\delta_{\gamma}/\delta_{\gamma\mathrm{LUXqed}}$.

3   Conclusions

We have calculated the NLO QCD and EW corrections to Higgs boson production in association with W and Z bosons at the LHC at 13 TeV and with Higgs boson mass $M_{\mathrm{H}} = 125$ GeV for various PDFs using the HAWK Monte Carlo tool within the G_{μ}-scheme. The total cross sections and fiducial cross sections for the processes pp→W$^{\pm}$+H→lν$_{\mathrm{l}}$ +H and pp→Z+H→l^{+}l^{-}+H were given in Tables 1, 2, 3, 4, 5, and 6. The EW corrections to W^{+}(→ l^{+}ν$_{\mathrm{l}}$)H, W^{-}(→ l^{-}ν̄$_{\mathrm{l}}$)H and Z(→l^{+}l^{-})H productions decrease the total cross sections by about -7.4%, -7.3% and -5.1% respectively. The NLO QCD corrections to W^{+}(→ l^{+}ν$_{\mathrm{l}}$)H, W^{-}(→ l^{-}ν̄$_{\mathrm{l}}$)H and Z(→ l^{+}l^{-})H productions increase the total cross sections by about 17.5%, 17.0% and 17.0% respectively. Our photon-induced process fiducial cross sections in Tables 4, 5, and 6 agree well with the results of Ref. [9] in their Tables 5.7, 5.8, and 5.9; and our EW corrections in Tables 1–3, and 4–6 agree well with the results of Ref. [9] in their Tables 5.3-5.5 and 5.7-5.9. The PDF uncertainties of the photon-induced process cross sections are reduced significantly for NNPDF2.3qed, NNPDF3.0qed, MRS2004qed, and CT14QEDinc photon PDF sets after including the CMS 8 TeV data. Especially, the CMS data can have a very large impact in reducing the NNPDF photon PDF errors.

References

1 For a review of the Higgs sector, see: J.F. Gunion, H.E. Haber, G.L. Kane and S. Dawson, The Higgs Hunter's Guide, Addison-Wesley, Reading 1990
2 T. Han, S. Willenbrock, FERMILAB-PUB-91/70-T, BNL-45990 (1991)
3 M. L. Ciccolini, S. Dittmaier, and M. Krämer, arXiv:hepph/0306234
4 O. Brein, M. Ciccolini, S. Dittmaier et al, arXiv: hepph/0402003
5 J. Pumplin, D. R. Stump, J. Huston et al, JHEP, **0207**: 012 (2002) arXiv: hepph/0201195
6 O. Brein , A. Djouadi, and R. Harlander, arXiv:hepph/0307206
7 A.D. Martin, R.G. Roberts, W.J. Stirling *et al.*, Phys. Lett. B, 531:216-224(2002)
8 A. Denner, S. Dittmaier, S. Kallweit et al, arXiv:1112.5142
9 The Working Group for standard model Higgs-Boson Searches, LHCHXSWG-DRAFT-INT-2016-008.
10 Mamut Ababekri, Sayipjamal Dulat, Joshua Isaacson et al, arXiv: 1603.04874
11 R. D. Ball et al (NNPDF Collaboration), JHEP, **1504**: 040 (2015) arXiv:1410.8849
12 C. Schmidt, J. Pumplin, D. Stump et al, arXiv:1509.02905
13 A. Manohar, P. Nason, G. P. Salam et al, arXiv:1607.04266
14 http://omnibus.uni-freiburg.de/sd565/programs/hawk/hawk.html, 2010
15 W. T. Giele and S. Keller, Phys. Rev. D, **58**: 094023 (1998) arXiv:hepph/9803393
16 R. D. Ball et al (NNPDF Collaboration), Nucl. Phys. B, **849**: 112 (2011) Erratum: [Nucl. Phys. B, **854**: 926 (2012)] Erratum: [Nucl. Phys. B, **855**: 927 (2012)] arXiv:1012.0836
17 R. D. Ball et al, Nucl. Phys. B, **855**: 608 (2012) arXiv:1108.1758
18 N. Sato, J. F. Owens, and H. Prosper, Phys. Rev. D, **89**(11): 114020 (2014)
19 V. Khachatryan et al (CMS Collaboration), arXiv:1604.04464